

# Synergistic effects of eukaryotic co-expression plasmid-based STAT3-specific siRNA and LKB1 on ovarian cancer *in vitro* and *in vivo*

YUAN PAN, LIQUN ZHANG, XINYUE ZHANG and RUIZHI LIU

Center for Reproductive Medicine, The First Hospital of Jilin University, Changchun, Jilin 130021, P.R. China

Received August 14, 2014; Accepted October 21, 2014

DOI: 10.3892/or.2014.3623

**Abstract.** The signal transducer and activator of transcription 3 (STAT3) are ideal targets for ovarian cancer. Previous studies showed that downregulation of STAT3 using specific short hairpin RNAs (shRNA) can significantly reduce ovarian tumor growth. However, RNA interference does not fully ablate target gene expression due to idiosyncrasies associated with shRNAs and their targets. To enhance the therapeutic efficacy of STAT3-specific shRNA, we employed a combinatorial expression of STAT3-specific shRNA and liver kinase B1 (*LKB1*), a tumor suppressor. Thus, the *LKB1* coding sequences and STAT3-specific shRNAs were constructed in a eukaryotic co-expression plasmid pCDNA3.1, and then transfected into ovarian cancer cells to evaluate the synergistic effects of this combination on anticancer activity and explore the relevant molecular mechanisms. Co-expression of STAT3-specific siRNA and *LKB1* (pSi-STAT3-*LKB1*) synergistically inhibited ovarian cancer cell growth, invasion and migration, induced cell apoptosis and arrested the cell cycle *in vitro* when compared with monotherapy. The results showed that the co-expression of plasmid pSi-STAT3-*LKB1* inserted subcutaneously into ovarian tumor xenograft resulted in more significant inhibition of tumor growth. Further study showed that the synergistic anti-ovarian cancer effects of the co-expression of STAT3-specific siRNA and *LKB1* may be associated with the upregulation of p-p53, p21 and downregulation of survivin, BCL-2 and cyclin D1. Results of the present study suggested that combined therapy with eukaryotic co-expression of the plasmid-carrying STAT3-specific siRNA and *LKB1* is a novel and efficient treatment strategy for human ovarian cancer.

## Introduction

Ovarian cancer is the fourth most lethal cancer among women and the leading cause of gynecological cancer-related deaths worldwide (1). Ovarian cancer is usually diagnosed at an advanced stage due to the asymptomatic nature of the early disease. The current standard therapy for ovarian cancer is surgical resection followed by adjuvant chemotherapy (2). Despite the increased use of surgery and chemotherapy to treat ovarian cancer, long-term survival for advanced stage ovarian cancer remains at  $\leq 20\text{-}30\%$  (3). This low survival rate is largely due to the presence of chemotherapy-resistant residual tumor cells which have the capacity to withstand the cytotoxic effects of therapies and repopulate, leading to recurrence (4). Therefore, the development of novel and effective therapeutic strategies for improving the prognosis of patients with ovarian cancer is necessary. Gene therapy is an attractive alternative compared with conventional therapies.

Signal transducers and activators of transcriptions (STATs) are a novel class of transcription factors that are positively associated with the cell growth and survival (5). STAT3, a member of the STAT family, is involved in the regulation of cell proliferation, differentiation, early embryonic development, apoptosis, cell migration and invasion, angiogenesis and immune responses (6-8). Following phosphorylation and activation, STAT3 dimers translocate into the nucleus, where they bind to specific DNA response elements in the promoter of target genes and activate their expression which is involved in various physiologic functions, including cell development, differentiation, proliferation and survival (8). In normal cells, STAT3 protein activation is strictly controlled to prevent unscheduled gene regulation. However, the constitutive activation of STAT3 and its overexpression have been detected in numerous human cancer cell lines and primary tumors, such as multiple myelomas, head and neck and ovarian cancer, leukemia, prostate, pancreatic, lung, gastric, as well as breast cancer (9-17).

Constitutively activated STAT3 is causally associated with tumor development and progression in a variety of solid malignancies including ovarian cancer (5,18,19). It has been showed that STAT3 activation is important in ovarian cancer growth and survival and resistance to chemotherapy (5). Since persistently activated STAT3 is involved in proliferation, survival and the migration of ovarian cancer cells, it is an attractive

---

*Correspondence to:* Professor Ruizhi Liu, Center for Reproductive Medicine, The First Hospital of Jilin University, Changchun, Jilin 130021, P.R. China  
E-mail: liuruizhi813@163.com

**Key words:** ovarian cancer, co-expression plasmid, gene silencing, STAT3, *LKB1*

target for intervention. Han *et al* (20) reported that targeting STAT3 by siRNA technology markedly enhanced cisplatin-induced apoptosis in cisplatin-resistant ovarian cancer cells that expressed a high level of pSTAT3. Findings of a recent study showed that depletion of STAT3 by siRNA causes the efficient inhibition of intraperitoneal ovarian cancer growth in nude mice (21). However, results of a previous study showed that blockade of STAT3 using short hairpin RNA (shRNA) expression vectors via a direct intrathecal (i.t.) injection did not identify a complete suppression of tumor growth in nude mice (22). It is well known that RNA interference does not completely block gene expression, particularly when the target mRNA is expressed at abnormally high levels (23). Therefore, whether another gene can be combined with shRNAs for enhanced suppression of tumor growth remains to be elucidated. The tumor suppressor, liver kinase B1 (*LKB1*) was therefore selected in this study.

*LKB1* is a candidate tumor-suppressor gene, located on chromosome 19p13.3 region, encoding an ~48 kDa multi-tasking kinase protein-*LKB1* (24). Altered *LKB1* expression has been associated with cancer development and growth (25). Recent studies have demonstrated that *LKB1* regulates cell growth, proliferation and survival in response to different stresses (24-27). Notably, it has been reported that *LKB1* inhibits the activation of STAT3 in cancer cell (28). Therefore, we selected *LKB1* combination with STAT3 shRNAs to enhance the suppression of ovarian tumor growth.

In the present study, the *LKB1* coding sequences and STAT3-specific shRNAs were constructed in a eukaryotic co-expression plasmid, and then transfected into ovarian cells to evaluate the therapeutic potential of the co-expression of STAT3-specific shRNAs and *LKB1*. Subsequently, the efficacy and mechanism of combination therapy with STAT3-specific shRNAs and *LKB1* for ovarian cancer *in vitro* and *in vivo* were investigated. The results suggested a novel strategy for ovarian cancer gene therapy.

## Materials and methods

**Reagents and antibodies.** The 3-(4,5-dimethylthiazol-2-yl)-2,5-diphenyltetrazolium bromide (MTT) solution was purchased from Sigma (St. Louis, MO, USA). Lipofectamine 2000 reagents, fetal bovine serum (FBS) and RPMI-1640 medium were purchased from Invitrogen (Carlsbad, CA, USA). Annexin V apoptosis detection kit I was obtained from BD Biosciences (BD Pharmingen, San Diego, CA, USA) and enhanced chemiluminescence (ECL) system from Amersham (Piscataway, NJ, USA). MMP-2 and MMP-9 antibodies were purchased from Abcam (Cambridge, UK). Anti-*LKB1* antibody was purchased from Upstate (Bedford, MA, USA). Antibodies against  $\beta$ -actin, P21, cyclin D1, STAT3, survivin and BCL-2 were obtained from Santa Cruz Biotechnology, Inc. (Santa Cruz, CA, USA). Antibodies against p-p53 were obtained from Cell Signaling Technology (Beverly, MA, USA).

**Cell lines and cell culture.** The human ovarian cancer cell lines, SKOV3, was purchased from the Cell Bank of Chinese Academy of Sciences (Shanghai, China). The cells were cultured in RPMI-1640 medium supplemented with 10% FBS,

100 IU/ml penicillin and 100  $\mu$ g/ml streptomycin (Gibco-BRL, Grand Island, NY, USA) in 5% CO<sub>2</sub> at 37°C.

**Plasmid construction and transfection.** Eukaryotic expression plasmid was constructed by pcDNA3.1 vector (Invitrogen) on request and as follows: the pcDNA3.1-siRNA-STAT3 (designated as pSi-STAT3) encoding siRNA specific to STAT3; pcDNA3.1-siRNA-Scramble plasmid (designated as pSi-Scramble, containing scrambled siRNA sequence) which served as a negative control; pcDNA3.1-LKB1 (designated as pLKB1) containing the *LKB1* coding region; and the co-expression plasmid pcDNA3.1-SiRNA-STAT3-LKB1 (designated as pSi-STAT3-LKB1) expressing the siRNA-STAT3 and *LKB1* gene.

SKOV3 cells were seeded at a density of  $3 \times 10^5$  cells/well in 6-well plates and allowed to adhere overnight. The cells were transfected with indicated plasmids using Lipofectamine 2000 (Invitrogen) according to the manufacturer's instructions for an additional 48-72 h prior to analysis of mRNA and protein expression levels, cell apoptosis and cell proliferation.

**Quantitative reverse transcription-PCR.** The mRNA expression levels of STAT3 and *LKB1* were examined using quantitative RT-PCR (RT-qPCR). In brief, SKOV3 cells were collected 48 h after transfection with various plasmids. Total RNA was extracted using the TRIzol reagent (Invitrogen). RNA was reverse-transcribed into cDNA by a PrimeScript™ RT reagent kit according to the manufacturer's instructions (Takara, Dalian, China). According to the cDNA sequences of *STAT3* and *LKB1* genes in the GenBank database, corresponding primers were designed and synthesized by Genomics Company (Guangzhou, China). The primers used for qPCR were: *STAT3*, forward: 5'-ACCTGCAGCAATACCATTGAC-3' and reverse: 5'-AAGGTGAGGGACTCAACTGC-3'; *LKB1*, forward: 5'-TGCTGAAAGGGATGCTTGAGTA-3' and reverse: 5'-GGATGGGCACTGGTGCTT-3'; and GAPDH, forward: 5'-CCACTCCTCCACCTTTGAC-3' and reverse: 5'-ACCCTGTTGCTGTAGCCA-3'. The primers were quantified by RT-qPCR using SYBR Premix *Ex* Taq (Takara). The RT-qPCR reactions were detected by SYBR Premix *Ex* Taq by using ABI 7900 Fast system (Applied Biosystems, Foster City, CA, USA). The expression levels of GAPDH were used as an internal control. PCR efficiencies were calculated with a relative standard curve derived from a complementary DNA mixture and yielded regression coefficients of >0.95. Quantification of gene expression was analyzed with the 7500 v 2.0.5 software program and quantified by the 2<sup>- $\Delta\Delta$ Ct</sup> method. All the experiments were repeated three times to reduce curve-derived variance.

**Western blot analysis.** For western blot analysis, after 48 h of transfection, the cells were collected and lysed by incubation on ice for 30 min in lysis buffer [25 mM Tris-HCl (pH 8.0), 1% Nonidet P-40, 0.5% sodium deoxycholate, 0.1% sodium dodecyl sulfate (SDS) and 125 mM NaCl] containing the complete protease inhibitor cocktail (Roche, Mannheim, Germany). Equal amounts of protein (20  $\mu$ g/lane) from the cell lysates were separated on 10% SDS-polyacrylamide gel (SDS-PAGE) and transferred onto nitrocellulose membranes (Santa Cruz Biotechnology, Inc.). The membrane was incubated for 2 h in PBS plus 0.1% Tween-20 and 5% non-fat skim milk to block

non-specific binding. The membranes were incubated with different primary antibodies overnight at 4°C and then incubated with the anti-mouse horseradish peroxidase-conjugated IgG (1:10,000; Santa Cruz Biotechnology, Inc.) for 1 h at room temperature. Immunoreactive complexes were detected with the ECL chemiluminescence detection system following the manufacturer's instructions. The band density was measured using the Quantity One software (Bio-Rad, Hercules, CA, USA) and normalized against the density of  $\beta$ -actin.

**Cell proliferation and colony formation.** Cell viability was determined using MTT assay as previously described (29). SKOV3 cells were transfected with different plasmids 24, 48 and 72 h after transfection, and the cell viability was quantified in a microplate reader (Molecular Devices Corporation, Sunnyvale, CA, USA) according to the manufacturer's instructions. Absorbance was measured at 570 nm and growth inhibition was subsequently calculated. The mean proliferation of cells without any treatment was expressed as 100%.

For the colony formation assay, SKOV3 cells transfected with different plasmids were seeded in 6-well plates at a low density ( $1 \times 10^3$  cells/well), respectively, and then cultured for 7 days. The cells were fixed with 4% paraformaldehyde for 20 min and counted after staining with 1% crystal violet. The experiments were carried out in triplicate wells at least three times.

**Cell cycle distribution and apoptosis assay.** Flow cytometry was used to detect cell cycle distribution and apoptosis. Briefly, at 24 h after transfection, the cells were collected. For cell cycle analysis, the cells were incubated with 2  $\mu$ g/ml of RNase A in PBS (200  $\mu$ l) and 0.1  $\mu$ g/ml of PI (Sigma) in 0.6% Nonidet P-40 on ice for 30 min. The DNA contents of samples were immediately measured using a FACSCalibur™ flow cytometer (BD Biosciences). Cell apoptosis was detected using a commercially Annexin V-FITC detection kit (KeyGen, Nanjing, China) according to the manufacturer's instructions. Data of the cell cycle phase distribution and cell apoptosis were determined by using CellQuest software (BD Biosciences).

In addition, in the present study, we detected caspase-3, -8 and -9 activity by caspase colorimetric protease assay kits (Millipore Corporation, Billerica, MA, USA) following the manufacturer's instructions, as an additional indicator of apoptosis.

**Wound-healing assays.** SKOV3 cells were treated with indicated plasmids when SKOV3 cells reached 80-90% confluence in 24-well plates. After 24 h of treatment, linear scratch wounds were created on the confluent cell monolayers with a 200  $\mu$ l pipette tip. To stop cells from entering the cell cycle prior to wounding, cells were maintained in serum-free medium. Images were captured at 0 and 24 h to visualize migrating cells and wound healing. The migration rate was quantified by counting the migration cells in 10 random fields under a light microscope (Olympus, Tokyo, Japan) at a magnification of x200.

**Cell invasion assay.** The Transwell migration chambers (8- $\mu$ m pore filter) were coated with Matrigel (both from BD Biosciences) and incubated at 37°C for 4 h, allowing it to

solidify. After 24 h of treatment with indicated plasmids,  $4 \times 10^5$  SKOV3 cells suspended in serum-free RPMI-1640 medium were added to the upper chamber, and medium containing 10% FBS was added to the lower chamber as a chemoattractant. After 48 h, the non-invading cells were gently removed, and invasive cells located on the lower surface of the chamber were stained with 0.1% crystal violet in 20% methanol. Invasiveness was determined by counting the penetrating cells in random 10 fields under a Nikon phase-contrast microscope of view at x200 magnification.

**Tumor xenografts in nude mice.** Approximately 5- to 6-week-old female BALB/c nude mice were purchased from the Jilin Institute of Experimental Animals. The research protocol was approved and mice were maintained in accordance with the Institutional Guidelines of the Experimental Animals of Jilin University. The mice were acclimatized for 1 week prior to being injected with cancer cells and injected subcutaneously with  $5 \times 10^6$  cells that had been resuspended in 200  $\mu$ l of Matrigel (Sigma). Tumor size was measured every 2-3 days, and tumor volume was calculated as  $0.5236 \times \text{width}^2 \times \text{length}$ . When established tumors of  $\sim 75 \text{ mm}^3$  in diameter were detected, 50 mice were randomly divided into five groups: i) control, ii) pSi-Scramble, iii) pSi-STAT3, iv) pLKB1 and v) pSi-STAT3-LKB1. In the control group, cells were inoculated with 50  $\mu$ l injection of PBS, while the remaining groups were inoculated with 20  $\mu$ g/50 $\mu$ l/mouse via i.t. injection of plasmids pSi-Scramble, pSi-STAT3, pLKB1 and pSi-STAT3-LKB1, respectively. Injection was performed once every 3 days. The mice were sacrificed on day 30, and tumor tissues were resected. Tumor volume and weight were measured and analyzed by western blotting for the expression of STAT3 and LKB1. In addition, spleen tissues were collected and cultured for a splenocyte surveillance study by MTT assay, as previously described (30).

**Statistical analysis.** Data from at least three independent experiments were presented as means  $\pm$  SD. The significant difference of the experimental results was calculated using one-way ANOVA followed by the Tukey's test. All the data were analyzed using the SPSS® statistical package, version 16.0 (SPSS, Inc., Chicago, IL, USA) and the GraphPad Prism version 5.01 (GraphPad Software, San Diego, CA, USA) for Windows®.  $P < 0.05$  was considered to indicate a statistically significant result.

## Results

**Effect of co-expression of pSi-STAT3-LKB1 plasmid on mRNA and protein expression of STAT3 and LKB1.** The pSi-STAT3, pLKB1 and pSi-STAT3-LKB1 plasmids, capable of expressing a shRNA that targets the STAT3, tumor suppressor LKB1 alone or in both, was constructed and then transfected into SKOV3 cells. STAT3 and LKB1 mRNA and protein expression levels were determined using RT-qPCR and western blotting, respectively. STAT3 expression levels of mRNA and protein were significantly decreased, while those of LKB1 were significantly upregulated following transfection with pLKB1, pSi-STAT3 and pSi-STAT3-LKB1 compared to the untreated and pSi-Scramble groups (Fig. 1A and B). Co-expression of

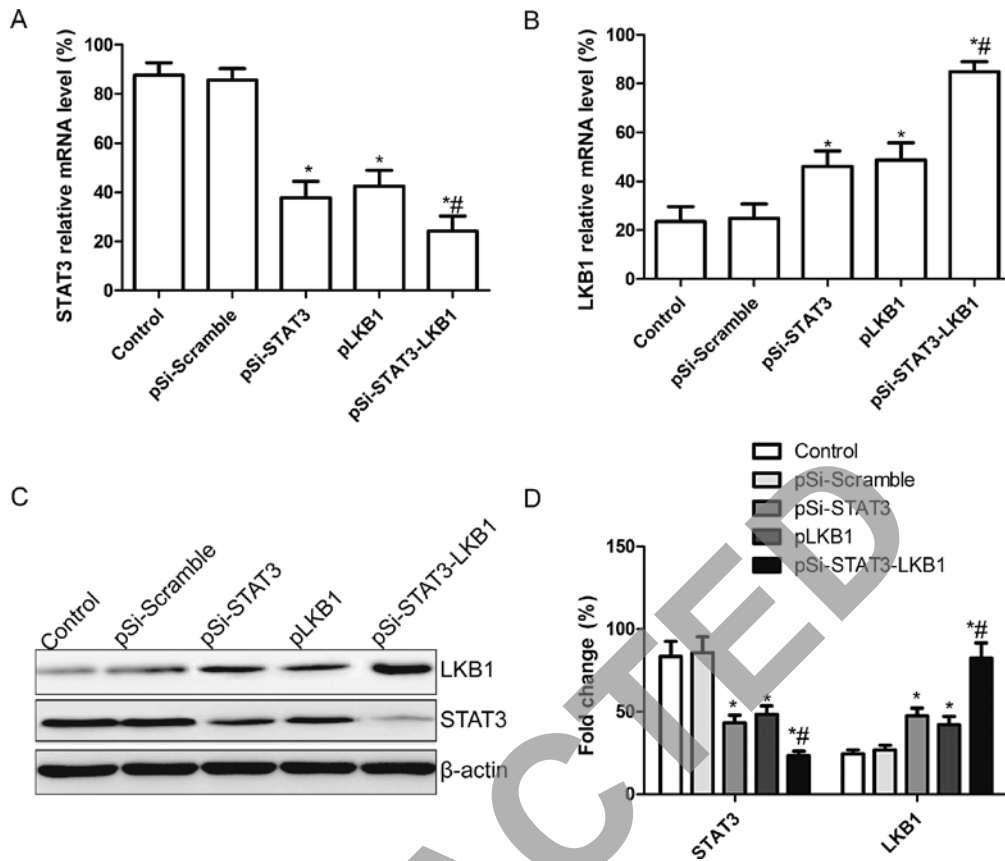


Figure 1. STAT3 and LKB1 mRNA and corresponding protein levels in SKOV3 cells transfected with different recombinant treatment plasmids. Quantitative RT-PCR (RT-qPCR) analysis of (A) STAT3 mRNA and (B) LKB1 mRNA in SKOV3 cells transfected with different recombinant treatment plasmids. (C) Western blot analysis for STAT3 and LKB1 in SKOV3 cells transfected with different recombinant treatment plasmids. (D) Quantification of STAT3 and LKB1 protein expression in SKOV3 cells transfected with different recombinant treatment plasmids. \*P<0.05 vs. control, #P<0.05 vs. pSi-STAT3 alone. STAT3, signal transducers and activators of transcription 3; LKB1, liver kinase B1.

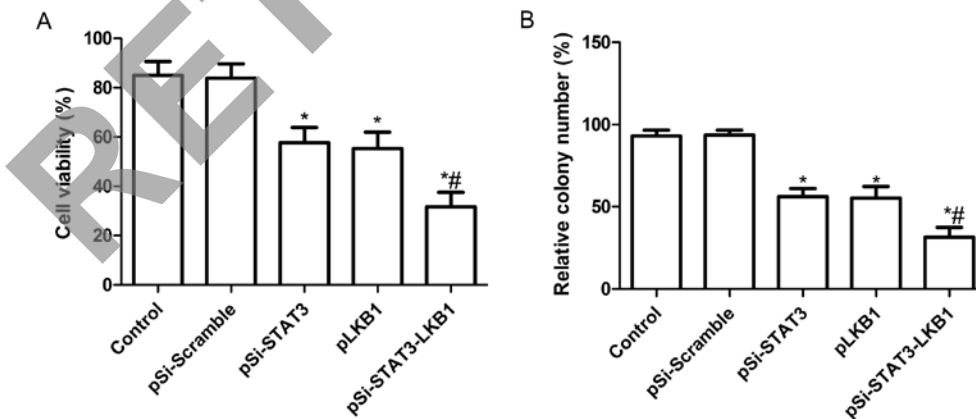


Figure 2. Cell proliferation and cell colony formation in SKOV3 cells transfected with different recombinant treatment plasmids. (A) Cell viability was determined by MTT assay in SKOV3 cells transfected with indicated plasmids. (B) Cell colony formation was detected in SKOV3 cells transfected with indicated plasmids. Assays were performed in triplicate. \*P<0.05 vs. control, #P<0.05 vs. pSi-STAT3 alone.

plasmid treatment exhibited a strong effect on STAT3 and LKB1 expression compared to single plasmid treatment as shown by western blotting and RT-qPCR (Fig. 1C and D).

*Synergistic effect of pSi-STAT3-LKB1 plasmid on cell proliferation and colony formation in SKOV3 cells.* To investigate whether pSi-STAT3, pLKB1 and pSi-STAT3-LKB1 plasmids

exert significantly different effects on cell proliferation, an MTT assay was performed 72 h after SKOV3 cells were transfected with individual plasmid. Fig. 2A shows that inhibition of cell proliferation was observed in SKOV3 cells transfected with pSi-Stat3 or pLKB1 individually. Co-expression of pSi-STAT3-LKB1 plasmid showed a greater synergistic inhibitory effect than individual pSi-STAT3 or pLKB1.

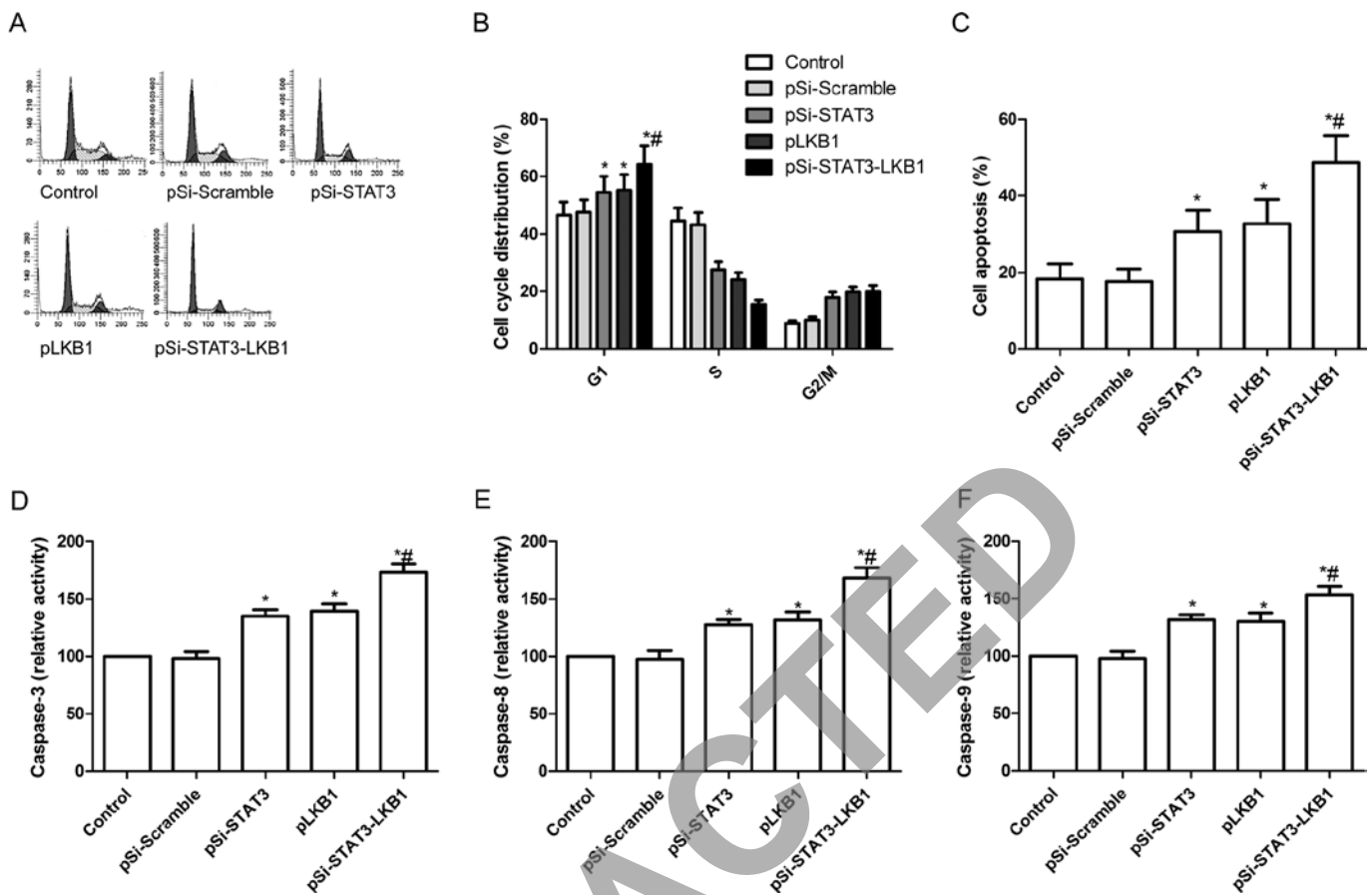


Figure 3. Cell cycle distribution and cell apoptosis in SKOV3 cells transfected with different recombinant treatment plasmids. (A) Cell DNA content distribution in each phase. (B) Percentage of cells distributed in each phase of the cell cycle. (C) Cell apoptosis was detected in SKOV3 cells transfected with indicated plasmids. (D) Caspase-3, (E) caspase-8 and (F) caspase-9 activity was determined in SKOV3 cells transfected with indicated plasmids. \* $P < 0.05$  vs. control, # $P < 0.05$  vs. pSi-STAT3 alone.

The effects of the co-expression of shRNA-STAT3 and LKB1 on tumor cell colony formation were determined in SKOV3 cell lines by analyzing cells colony formation at 14 days after transfection. It was found that cell colony formation in the pSi-STAT3, pLKB1 and pSi-STAT3-LKB1 groups was significantly reduced compared to the control and pSi-Scramble groups ( $P < 0.05$ ; Fig. 2B). Among the SKOV3 cell groups treated with pSi-STAT3, pLKB1 and pSi-STAT3-LKB1, the lowest incidence of cell colony formation was observed in the pSi-STAT3-LKB1 treatment group. No significant difference was identified between the pSi-STAT3 and pLKB1 groups ( $P > 0.05$ ).

**Synergistic effect of pSi-STAT3-LKB plasmid on cell cycle and apoptosis in SKOV3 cells.** To determine the effects of pSi-STAT3, pLKB1 and pSi-STAT3-LKB1 plasmids on the cell cycle, FACSscan flow cytometry assays were performed and the results showed that pSi-STAT3 or pLKB1 was arrested in the G0/G1 phase compared to the control and pSi-Scramble groups ( $P < 0.05$ , Fig. 3A and B). However, the effects of this arrest were weaker as compared to the cells transfected with pSi-STAT3-LKB1 ( $P < 0.05$ , Fig. 3A and B).

To study the effect of co-expression of pSi-STAT3-LKB1 plasmid on cell apoptosis, flow cytometry was used. Fig. 3C shows that apoptosis was evident in SKOV3 cells transfected with pSi-STAT3 (30.6%) or pLKB1 (32.7%) individually,

however, significant enhancement of apoptosis was observed in SKOV3 cells transfected with pSi-STAT3-LKB1 (48.7%).

To determine the potential mechanism of cell growth inhibition *in vitro*, caspase-3, -8 and -9 activity was detected using ELISA. We found that caspase-3, -8 and -9 activity was significantly increased in pSi-STAT3, pLKB1 and pSi-STAT3-LKB1 treatment groups compared to the control and pSi-Scramble groups ( $P < 0.05$ ; Fig. 3D-F). Furthermore, the group transfected with plasmid pSi-STAT3-LKB1 showed the greatest increase (Fig. 3D-F).

**Synergistic effect of pSi-STAT3-LKB1 plasmid on cell migration and invasion in SKOV3 cells.** To determine the effect of the co-expression of pSi-STAT3-LKB1 plasmid on the migration of SKOV3 cells, a wound-healing assay was performed. The results showed that pSi-STAT3 and pLKB1 caused a decrease in SKOV3 cell migration, although significant synergistic inhibition of invasion was observed in SKOV3 cells transfected with co-expression of the pSi-STAT3-LKB1 plasmid ( $P < 0.05$ ; Fig. 4A and B).

The ability of co-expression of the pSi-STAT3-LKB1 plasmid to reduce the invasiveness of ovarian cancer cells was subsequently investigated using the Transwell system assay. Cell invasion was decreased significantly in the pSi-STAT3, pLKB1 and the pSi-STAT3-LKB1 treatment group compared to the control and pSi-Scramble groups, whereas a synergistic

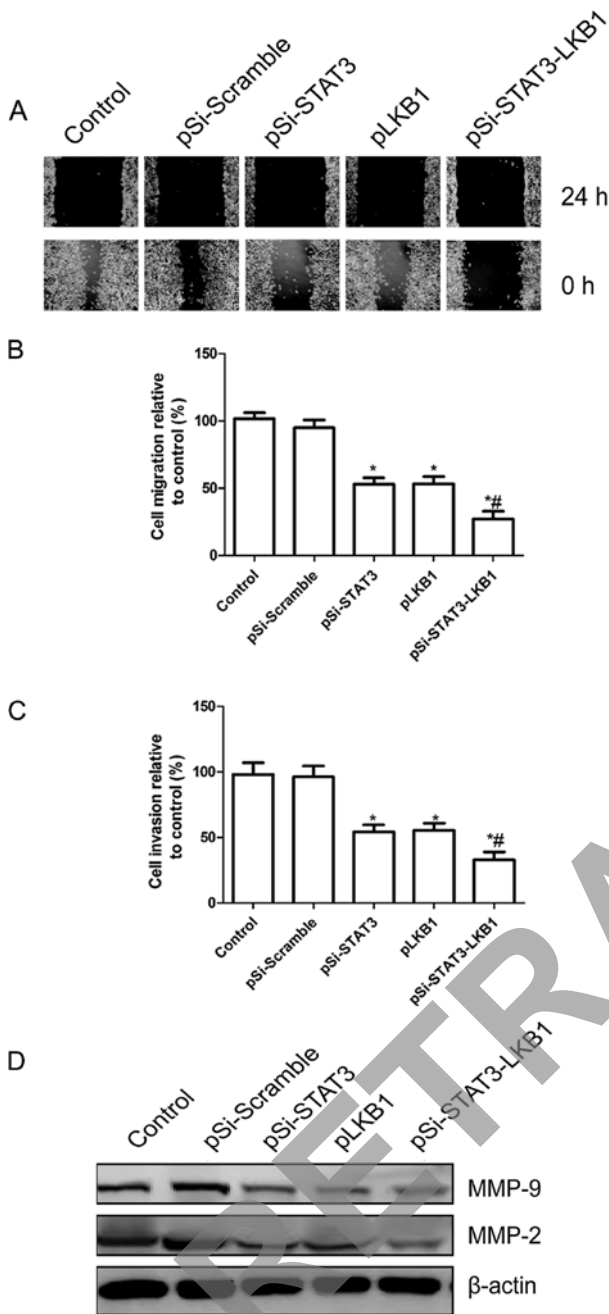


Figure 4. Cell migration and invasion in SKOV3 cells transfected with different recombinant treatment plasmids. (A) Representative images of migration in SKOV3 cells transfected with different recombinant treatment plasmids. (B) The number of migration cells was measured. (C) The number of invasion cells was counted in SKOV3 cells transfected with different recombinant treatment plasmids. (D) Western blot analysis was used to assess expression of MMP-2 and MMP-9 using corresponding antibodies.  $\beta$ -actin was used as an internal control. \* $P < 0.05$  vs. control, \*\* $P < 0.05$  vs. pSi-STAT3 alone.

inhibition of invasion was evident in SKOV3 cells transfected with co-expression of pSi-STAT3-LKB1 plasmid (Fig. 4C).

To determine the potential mechanism of cell migration inhibition and cell invasion inhibition *in vitro*, we examined the relevant effector molecules, including MMP-2 and MMP-9 by western blot analysis. Western blot analysis revealed a significantly decrease in MMP-2 and MMP-9 proteins in pSi-STAT3, pLKB1 and pSi-STAT3-LKB1 treatment groups compared to the control and pSi-Scramble groups (Fig. 4D).

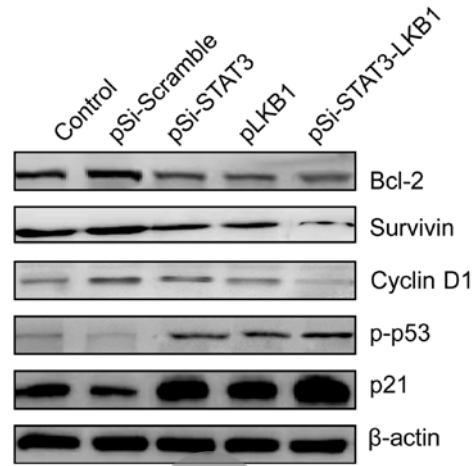


Figure 5. Effect of co-expression of pSi-STAT3-LKB1 plasmid on relevant tumor effector molecules *in vitro*. SKOV3 cells were transfected with different recombinant treatment plasmids. Non-transfection was used as a negative control. At 48 h after transfection, the cells were collected and protein levels of p21, p-p53, cyclin D1, survivin and Bcl-2 were analyzed by western blotting using specific antibodies.  $\beta$ -actin was used as an internal control.

The pSi-STAT3-LKB1 group showed maximally reduced expression compared to the pSi-STAT3 or pGRIM-19 groups (Fig. 4D). Collectively, these results suggested that the synergistic pSi-STAT3-LKB1 effects of on ovarian cancer cell migration and invasion were at least partially mediated by the downregulation of MMP-2 and MMP-9, which may contribute to the degradation of the extracellular matrix.

*Synergistic effect of co-expression the pSi-STAT3-LKB1 plasmid on relevant tumor effector molecules in vitro.* To elucidate the molecular mechanisms responsible for the synergistic growth inhibition and apoptotic induction of ovarian cancer cells by co-expression shRNA-STAT3 and LKB1, the expression of p21, p-p53, cyclin D1, survivin and Bcl-2 was detected in the ovarian cells transfected with indicated plasmids by western blot analysis. The expression levels of p-p53 and p21 proteins were upregulated, while cyclin D1, survivin and Bcl-2 were downregulated in SKOV3 cells transfected with pSi-STAT3, pLKB1 and pSi-STAT3-LKB1 plasmids (Fig. 5). Co-expression of pSi-STAT3-LKB1 plasmid resulted in further upregulation of p-p53 and p21, and downregulation of cyclin D1, survivin and Bcl-2 at protein levels compared to the pSi-STAT3 or pLKB1 group (Fig. 5).

*Synergistic effect of co-expression of pSi-STAT3-LKB1 plasmid on tumor growth in vivo.* To determine the synergistic tumor suppressive function mediated by the co-expression of shRNA-STAT3 and LKB1 *in vivo*, the combined effects on tumor growth were investigated in the xenograft tumor model. Tumor growth was monitored for 30 days. On day 30, animals were sacrificed and tumor weight and volume were measured. Tumor weight and volume of mice treated with pSi-STAT3, pLKB1 and pSi-STAT3-LKB1 were significantly reduced when compared to the control and pSi-Scramble groups ( $P < 0.05$ ; Fig. 6A-C). Moreover, the inhibition of tumor growth in the pSi-STAT3-LKB1 group was more evident than in the pSi-STAT3 and pLKB1 groups ( $P < 0.05$ ; Fig. 6A-C).

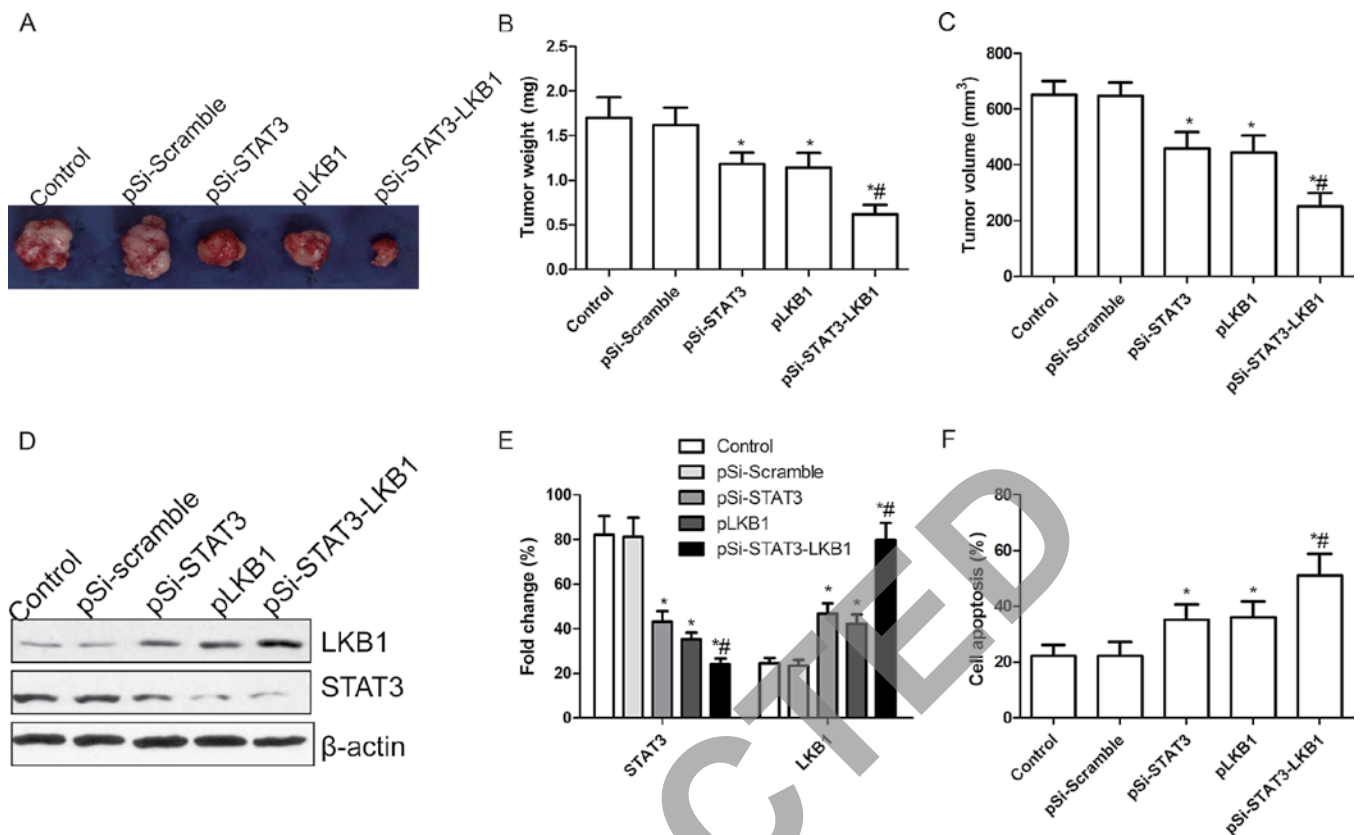


Figure 6. Inhibition of tumor growth in BALB/c mice bearing SKOV3 cells by treatments with different recombinant treatment plasmids. (A) Images of tumor tissue with different plasmid treatments collected after sacrifice at day 30. (B) Tumor wet weights were measured after sacrifice at day 30. (C) Tumor volume was measured after sacrifice at day 30. (D) Western blot analysis for STAT3 and LKB1 in tumor tissues following treatment with various plasmids. (E) Quantification of STAT3 and LKB1 protein expression in tumor tissue following treatment with different recombinant treatment plasmids. (F) MTT assay of cell proliferation of splenocytes from mice following treatment with various plasmids. \* $P < 0.05$  vs. control, # $P < 0.05$  vs. pSi-STAT3 alone. LKB1, liver kinase B1.

We also examined the expression of STAT3 and LKB1 in grafted tumor tissues by western blot analysis. The results showed that LKB1 expression levels were obviously increased, while STAT3 expression had a marked decrease in the groups treated with pSi-STAT3, pLKB1 and pSi-STAT3-LKB1 ( $P < 0.05$ ; Fig. 6D and E). Co-expression of pSi-STAT3-LKB1 plasmid group was enhanced compared to the pSi-STAT3 and pLKB1 groups. Apart from measuring the tumor volumes, we employed MTT assays to modulate splenocyte proliferation to demonstrate the antitumor activities. As shown in Fig. 6F, cell proliferation of pSi-STAT3, pLKB1 and pSi-STAT3-LKB1 was significantly increased compared to control and pSi-Scramble group ( $P < 0.01$ ). Treatment with pSi-STAT3-LKB1 resulted in a marked reduction in cell proliferation as compared to pSi-STAT3 and pLKB1 ( $P < 0.05$ , Fig. 6F). These results suggested that co-expression of the pSi-STAT3-LKB1 plasmid produced a synergistic and more effective therapeutic efficacy for suppressing ovarian tumor growth in the mouse model.

## Discussion

It is well known that gene therapy targeting human STAT3 or LKB1 alone causes tumor growth inhibition. However, to the best of our knowledge, the present findings are the first to show that combinatorial gene therapy targeting shRNA-STAT3 and LKB1 causes additive effects on ovarian cell proliferation, colony formation, cycle distribution, apoptosis, migration and

invasion *in vitro*, as well as on tumor growth inhibition *in vivo*. This is a new strategy that may be adopted in the clinic and result in improved therapeutic outcome for the treatment of ovarian cancer.

Cancer is caused by multiple factors, rendering the single gene therapy a challenge. Therefore, combinatorial gene therapy by targeting several signaling pathways involved in the proliferation and survival of cancer cells is becoming a new hot field of research. Extensive studies have shown that combined gene therapy can kill tumor cells by synergistically targeting several genes involved in tumor occurrence and/or development (22,29,31,32). STAT3 has been identified as an oncogene that is frequently activated in various cancer cells, including ovarian cancer (5,18,19). It has been shown that the shRNA-STAT3 gene alone or shRNA-STAT3 combined with other genes inhibited tumor growth (5,18,19,22,29,32). In particular, shRNA-STAT3 combined with other tumor-suppressor genes have additive effects on the inhibition of tumor growth compared to single gene therapy. For example, findings of a recent study showed that co-expressed STAT3-specific shRNA and GRIM-19 synergistically and more effectively suppressed tumor growth of thyroid growth *in vitro* and *in vivo* compared to single gene treatment (29). Zhang *et al* also reported similar findings in prostate tumor growth (22). Moreover, several studies have provided strong evidence that LKB1 loss promotes the carcinogenic process, such as cell apoptosis, cycle regulation, tumor angiogenesis and metastasis (24-27). Overexpression of

LKB1 alone or combination with other tumor-suppressor genes inhibited tumor growth. Li *et al* reported that combined therapy with eukaryotic co-expression of plasmid carrying *LKB1* and *FUS1* genes inhibited NSCLC cell growth *in vitro* and *in vivo* by targeting multiple signaling pathways (33). Notably, it has been demonstrated that the downregulation of LKB1 expression increases STAT3 activity, which may promote tumor growth during esophageal cancer progression (28). Therefore, we selected LKB1 combination with shRNA-STAT3 to enhance the suppression of ovarian tumor growth. We found that simultaneous expression of STAT3-specific shRNA and LKB1 in SKOV3 cells significantly suppressed ovarian tumor growth *in vitro* and *in vivo*, when compared to single gene therapy. Our findings along with those of other studies suggest that combined gene therapy may be a more effective method with regard to single gene therapy.

The exact mechanism behind the additive effects remains to be clarified. Findings of previous studies may prove useful. LKB1 inhibits tumor cell cycle progression by inducing p21 and p53 gene expression which is dependent on its kinase activity (34,35). LKB1 deficiency leads to the induction of MMP-2 and MMP-9 (36). These genes are all regulated by STAT3 and are involved in cell growth, tumorigenesis and angiogenesis (6,8). In addition, LKB1 suppresses tumor growth by inhibiting the activation of oncogenic STAT3 in papillary thyroid carcinoma (36) and esophageal cancer (28). Therefore, we hypothesize that the expression of STAT3-specific shRNA and LKB1 causes an additive effect on cell cycle and apoptosis via the regulation of genes including cyclin D1, p21, p-p53, survivin and Bcl-2. In the present study, to test this hypothesis, the expression of p-p53, p21, cyclin D1, survivin and Bcl-2 was detected by western blot analysis. The results show that co-expression of pSi-STAT3-LKB1 plasmid upregulated the expression of p21 and p-p53 and markedly downregulated the expression of cyclin D1, survivin and Bcl-2 in SKOV3 cells. Thus, the molecular mechanism of the co-expression of shRNA-STAT3 and LKB1 on inducing cell apoptosis and arresting cell cycle in ovarian cancer cell lines may be associated with the upregulation of p-p53 and p21 and downregulation of cyclin D1, survivin and Bcl-2.

Downregulation of MMP-2 and MMP-9 is known to contribute to the inhibition of cancer cell invasion and metastasis (37). Recent studies have shown that the overexpression of LKB1 in cancer cells inhibited cell migration and invasion, which were associated with the downregulation of MMP-2 and MMP-9 (36,38). In addition, silencing STAT3 has been found to inhibit cancer cell migration and invasion via the downregulation of MMP-2 and MMP-9 expression (29). To examine the molecular mechanism of the synergistic effect of co-expression of shRNA-STAT3 and LKB1 on ovarian cancer cell migration and invasion, we evaluated the protein expression of MMP-2 and MMP-9 in SKOV3 cells transfected with the indicated plasmids. Our results show that co-expressed STAT3-specific shRNA and LKB1 synergistically suppressed ovarian cancer cell migration and invasion via the downregulation of MMP-2 and MMP-9 expression, which may contribute to the degradation of the extracellular matrix.

In conclusion, our data have demonstrated that simultaneous expression of shRNA-STAT3 and LKB1 (pSi-STAT3-LKB1) in SKOV3 cells synergistically inhibited cell

proliferation, colony formation, migration and invasion and induced cell cycle and cell apoptosis *in vitro*, and suppressed tumor growth in a mouse model. These findings suggest that co-expression of shRNA-STAT3 and LKB1 in the same eukaryotic co-expression plasmid vector may be a novel and effective therapeutic strategy for human ovarian cancer.

## References

1. Siegel R, Naishadham D and Jemal A: Cancer statistics, 2012. *CA Cancer J Clin* 62: 10-29, 2012.
2. Cannistra SA: Cancer of the ovary. *N Engl J Med* 351: 2519-2529, 2004.
3. Kipps E, Tan DS and Kaye SB: Meeting the challenge of ascites in ovarian cancer: new avenues for therapy and research. *Nat Rev Cancer* 13: 273-282, 2013.
4. Telleria CM: Repopulation of ovarian cancer cells after chemotherapy. *Cancer Growth Metastasis* 6: 15-21, 2013.
5. Duan Z, Foster R, Bell DA, *et al*: Signal transducers and activators of transcription 3 pathway activation in drug-resistant ovarian cancer. *Clin Cancer Res* 12: 5055-5063, 2006.
6. Darnell JE Jr: STATs and gene regulation. *Science* 277: 1630-1635, 1997.
7. Lu Y, Fukuyama S, Yoshida R, *et al*: Loss of SOCS3 gene expression converts STAT3 function from anti-apoptotic to pro-apoptotic. *J Biol Chem* 281: 36683-36690, 2006.
8. Yu H and Jove R: The STATs of cancer - new molecular targets come of age. *Nat Rev Cancer* 4: 97-105, 2004.
9. Catlett-Falcone R, Landowski TH, Oshiro MM, *et al*: Constitutive activation of Stat3 signaling confers resistance to apoptosis in human U266 myeloma cells. *Immunity* 10: 105-115, 1999.
10. Grandis JR, Drenning SD, Zeng Q, *et al*: Constitutive activation of Stat3 signaling abrogates apoptosis in squamous cell carcinogenesis *in vivo*. *Proc Natl Acad Sci USA* 97: 4227-4232, 2000.
11. Yan X, Fraser M, Qiu Q and Tsang BK: Over-expression of PTEN sensitizes human ovarian cancer cells to cisplatin-induced apoptosis in a p53-dependent manner. *Gynecol Oncol* 102: 348-355, 2006.
12. Epling-Burnette PK, Liu JH, Catlett-Falcone R, *et al*: Inhibition of STAT3 signaling leads to apoptosis of leukemic large granular lymphocytes and decreased Mcl-1 expression. *J Clin Invest* 107: 351-362, 2001.
13. Mora LB, Buettner R, Seigne J, *et al*: Constitutive activation of Stat3 in human prostate tumors and cell lines: direct inhibition of Stat3 signaling induces apoptosis of prostate cancer cells. *Cancer Res* 62: 6659-6666, 2002.
14. Scholz A, Heinze S, Detjen KM, *et al*: Activated signal transducer and activator of transcription 3 (STAT3) supports the malignant phenotype of human pancreatic cancer. *Gastroenterology* 125: 891-905, 2003.
15. Song L, Turkson J, Karras JG, Jove R and Haura EB: Activation of Stat3 by receptor tyrosine kinases and cytokines regulates survival in human non-small cell carcinoma cells. *Oncogene* 22: 4150-4165, 2003.
16. Kanda N, Seno H, Konda Y, *et al*: STAT3 is constitutively activated and supports cell survival in association with survivin expression in gastric cancer cells. *Oncogene* 23: 4921-4929, 2004.
17. Li L and Shaw PE: Autocrine-mediated activation of STAT3 correlates with cell proliferation in breast carcinoma lines. *J Biol Chem* 277: 17397-17405, 2002.
18. Aittomäki S and Pesu M: Therapeutic targeting of the Jak/STAT pathway. *Basic Clin Pharmacol Toxicol* 114: 18-23, 2014.
19. Huang K, Li LA, Meng YG, You YQ, Fu XY and Song L: Arctigenin promotes apoptosis in ovarian cancer cells via the iNOS/NO/STAT3/survivin signalling. *Basic Clin Pharmacol Toxicol*: May 19, 2014 (Epub ahead of print). doi: 10.1111/bcpt.12270.
20. Han Z, Feng J, Hong Z, *et al*: Silencing of the STAT3 signaling pathway reverses the inherent and induced chemoresistance of human ovarian cancer cells. *Biochem Biophys Res Commun* 435: 188-194, 2013.
21. Jiang Q, Dai L, Cheng L, *et al*: Efficient inhibition of intraperitoneal ovarian cancer growth in nude mice by liposomal delivery of short hairpin RNA against STAT3. *J Obstet Gynaecol Res* 39: 701-709, 2013.

22. Zhang L, Gao L, Li Y, *et al*: Effects of plasmid-based Stat3-specific short hairpin RNA and GRIM-19 on PC-3M tumor cell growth. *Clin Cancer Res* 14: 559-568, 2008.
23. Elbashir SM, Harborth J, Weber K and Tuschl T: Analysis of gene function in somatic mammalian cells using small interfering RNAs. *Methods* 26: 199-213, 2002.
24. Hemminki A, Markie D, Tomlinson I, *et al*: A serine/threonine kinase gene defective in Peutz-Jeghers syndrome. *Nature* 391: 184-187, 1998.
25. Esteller M, Avizienyte E, Corn PG, *et al*: Epigenetic inactivation of *LKB1* in primary tumors associated with the Peutz-Jeghers syndrome. *Oncogene* 19: 164-168, 2000.
26. Andrade-Vieira R, Xu Z, Colp P and Marignani PA: Loss of *LKB1* expression reduces the latency of ErbB2-mediated mammary gland tumorigenesis, promoting changes in metabolic pathways. *PLoS One* 8: e56567, 2013.
27. Zhuang Z, Wang K, Cheng X, *et al*: LKB1 inhibits breast cancer partially through repressing the Hedgehog signaling pathway. *PLoS One* 8: e67431, 2013.
28. Wang YQ, Dai WM, Chu XY, Yang B, Zhao M and Sun Y: Downregulation of LKB1 suppresses Stat3 activity to promote the proliferation of esophageal carcinoma cells. *Mol Med Rep* 9: 2400-2404, 2014.
29. Wang GM, Ren ZX, Wang PS, *et al*: Plasmid-based Stat3-specific siRNA and GRIM-19 inhibit the growth of thyroid cancer cells *in vitro* and *in vivo*. *Oncol Rep* 32: 573-580, 2014.
30. Du Y, Shi A, Han B, *et al*: COX-2 silencing enhances tamoxifen antitumor activity in breast cancer *in vivo* and *in vitro*. *Int J Oncol* 44: 1385-1393, 2014.
31. Wen LJ, Gao LF, Jin CS, *et al*: Small interfering RNA survivin and GRIM-19 co-expression salmonella plasmid inhibited the growth of laryngeal cancer cells *in vitro* and *in vivo*. *Int J Clin Exp Pathol* 6: 2071-2081, 2013.
32. Li X, Li Y, Hu J, *et al*: Plasmid-based E6-specific siRNA and co-expression of wild-type p53 suppresses the growth of cervical cancer *in vitro* and *in vivo*. *Cancer Lett* 335: 242-250, 2013.
33. Li L, Yu C, Ren J, *et al*: Synergistic effects of eukaryotic co-expression plasmid carrying *LKB1* and *FUS1* genes on lung cancer *in vitro* and *in vivo*. *J Cancer Res Clin Oncol* 140: 895-907, 2014.
34. Tiainen M, Vaahtomeri K, Ylikorkala A and Mäkelä TP: Growth arrest by the LKB1 tumor suppressor: induction of p21<sup>WAF1/CIP1</sup>. *Hum Mol Genet* 11: 1497-1504, 2002.
35. Tiainen M, Ylikorkala A and Mäkelä TP: Growth suppression by Lkb1 is mediated by a G<sub>1</sub> cell cycle arrest. *Proc Natl Acad Sci USA* 96: 9248-9251, 1999.
36. Kim DW, Chung HK, Park KC, *et al*: Tumor suppressor LKB1 inhibits activation of signal transducer and activator of transcription 3 (STAT3) by thyroid oncogenic tyrosine kinase rearranged in transformation (RET)/papillary thyroid carcinoma (PTC). *Mol Endocrinol* 21: 3039-3049, 2007.
37. Braicu EI, Gasimli K, Richter R, *et al*: Role of serum VEGFA, TIMP2, MMP2 and MMP9 in monitoring response to adjuvant radiochemotherapy in patients with primary cervical cancer - results of a companion protocol of the randomized NOGGO-AGO phase III clinical trial. *Anticancer Res* 34: 385-391, 2014.
38. Ou W, Ye S, Yang W, *et al*: Enhanced antitumor effect of cisplatin in human NSCLC cells by tumor suppressor LKB1. *Cancer Gene Ther* 19: 489-498, 2012.

RETRACTED